



RESEARCH ARTICLE

# Observation of significant photosynthesis in garden cress and cyanobacteria under simulated illumination from a K dwarf star

Iva Vilović<sup>1</sup> , Dirk Schulze-Makuch<sup>1,2,3,4</sup> and René Heller<sup>5</sup> 

<sup>1</sup>Astrobiology Research Group, Zentrum für Astronomie und Astrophysik, Technische Universität Berlin, 10623 Berlin, Germany

<sup>2</sup>GFZ German Research Center for Geosciences, Section Geomicrobiology, 14473 Potsdam, Germany

<sup>3</sup>Department of Experimental Limnology, Leibniz-Institute of Freshwater Ecology and Inland Fisheries (IGB), 16775 Stechlin, Germany

<sup>4</sup>School of the Environment, Washington State University, Pullman, WA, USA

<sup>5</sup>Solar and Stellar Interiors, Max-Planck-Institut für Sonnensystemforschung, 37077 Göttingen, Germany

**Corresponding author:** Iva Vilović; Email: [iva.vilovic@campus.tu-berlin.de](mailto:iva.vilovic@campus.tu-berlin.de)

**Received:** 9 October 2023; **Revised:** 13 May 2024; **Accepted:** 27 May 2024

**Keywords:** exoplanets, K dwarf stars, starlight simulator, superhabitability

## Abstract

Stars with about 45 to 80% the mass of the Sun, so-called K dwarf stars, have previously been proposed as optimal host stars in the search for habitable extrasolar worlds. These stars are abundant, have stable luminosities over billions of years longer than Sun-like stars, and offer favourable space environmental conditions. So far, the theoretical and experimental focus on exoplanet habitability has been on even less massive, though potentially less hospitable red dwarf stars. Here we present the first experimental data on the responses of photosynthetic organisms to a simulated K dwarf spectrum. We find that garden cress *Lepidium sativum* under K-dwarf radiation exhibits comparable growth and photosynthetic efficiency as under Solar illumination on Earth. The cyanobacterium *Chroococcidiopsis* sp. CCMEE 029 exhibits significantly higher photosynthetic efficiency and culture growth under K dwarf radiation compared to Solar conditions. Our findings of the affirmative responses of these two photosynthetic organisms to K dwarf radiation suggest that exoplanets in the habitable zones around such stars deserve high priority in the search for extrasolar life.

## Contents

<b>Introduction</b>	<b>1</b>
<b>Results</b>	<b>2</b>
Garden cress ( <i>Lepidium sativum</i> )	2
Cyanobacterium ( <i>Chroococcidiopsis</i> sp. CCMEE 029)	6
<b>Discussion</b>	<b>7</b>
<b>Conclusion</b>	<b>10</b>
<b>Methods</b>	<b>11</b>
General experimental course	11
Model spectra	11
Creating the starlight simulator	11
Laboratory procedures	12

## Introduction

Light is the fundamental energy source for photosynthesis, enabling the synthesis of organic compounds. Over billions of years, photosynthetic organisms have profoundly transformed our planet

into a diverse global ecosystem (Kiang *et al.*, 2007a, 2007b). Therefore, understanding any planet in the context of its stellar environment is an essential step in assessing its habitability. The only life we know of so far has developed around our Sun – a G dwarf star in the Harvard spectral classification system with an effective temperature of 5770 K (Williams, 2013). In addition to the search for Earth-like planets around Sun-like stars, much of the focus in the search of extraterrestrial life (Anglada-Escudé *et al.*, 2016; Gillon *et al.*, 2016, 2017; Rajpurohit *et al.*, 2018; Gebauer *et al.*, 2021) has been placed on the smallest, least massive and coolest type of star. These red dwarf stars (M dwarfs) possess a range of favourable attributes that are conducive to the detection and potential development of life (Adams *et al.*, 2005). It has even been demonstrated that photosynthetic organisms from Earth can grow and photosynthesize under simulated M dwarf radiation, highlighting the potential viability of modified spectra for biological processes (Claudi *et al.*, 2020; Battistuzzi *et al.*, 2023a, 2023c). That being said, planets orbiting M dwarfs face challenges such as intense tidal forces (Barnes *et al.*, 2009; Heller *et al.*, 2011), significant water loss during the super luminous pre-main sequence phase (Luger and Barnes, 2015) and exposure to substantial levels of extreme UV radiation and high-energy particles. These factors can lead to the photochemical destruction of atmospheric biosignatures and atmospheric erosion (Scalo *et al.*, 2007; Barnes *et al.*, 2009).

In comparison, K dwarf stars are the second most abundant star-types in the Milky Way and their lifetimes vastly exceed the expected main-sequence lifetime of our Sun by billions of years (Zakhzhay, 2013; Arney, 2019). They are also magnetically less active than M dwarfs and thus show less frequent radiation outbursts and coronal mass ejections (Zakhzhay, 2013; Arney, 2019). Planets in the respective habitable zones of K dwarf stars experience up to 1000 times lower UV and X-ray fluxes compared to planets that orbit late M dwarf stars (Richey-Yowell *et al.*, 2019). Most importantly, the habitable zones of the majority of K dwarf stars, when considering their masses and temperatures, do not overlap with the range of distances where a planet in orbit would become tidally locked, preventing dramatic climate variations which could be detrimental for the emergence or sustenance of life (Dole and Henry, 1966; Peale, 1977; Kasting *et al.*, 1993; Barnes, 2017). Furthermore, K dwarf stars have shorter pre-main sequence phases – <0.1 Gyr in comparison to 1 Gyr for M dwarfs, and their FUV and X-ray fluxes weaken around six times faster than for M dwarf stars, which potentially allows for early habitability (Cuntz and Guinan, 2016; Arney, 2019). All things combined; K dwarfs can be considered the ‘Goldilocks stars’ in the search for potentially life-bearing planets. A comparison of all parameters between the Sun–Earth and K dwarf–exoplanetary systems used in this work can be found in Table 2 in the Methods section.

## Results

### **Garden cress (*Lepidium sativum*)**

We investigated the viability of simulated K dwarf radiation for the photosynthetic processes of garden cress *Lepidium sativum* and the cyanobacterial strain *Chroococcidiopsis sp. 029*. Figure 1 shows a top view visual growth comparison of garden cress under Solar, K dwarf and dark conditions for selected days after sowing the seeds. The garden cress under K dwarf radiation was visually comparable to garden cress under Solar radiation, most of the time even sprouting a day or two earlier.

It developed a vibrant green colour and visual inspection suggests that its leaf surface area appeared to be marginally larger compared to garden cress under Solar radiation. As expected, garden cress grown in continuous darkness also sprouted, but it did so with a delay, and it did not develop the green pigment indicative of photosynthesis. Once it sprouted, visual examination suggests that it grew higher than any of the illuminated samples.

A lateral perspective of the plant on the seventh day after seed sowing is shown in Fig. 2. Visual assessment suggests that there are notable differences in stem elongation and overall height of the garden cress grown under the three irradiation regimes. For example, observations suggest that garden cress under K dwarf radiation grew higher than under Solar light. As expected, the plant under constant

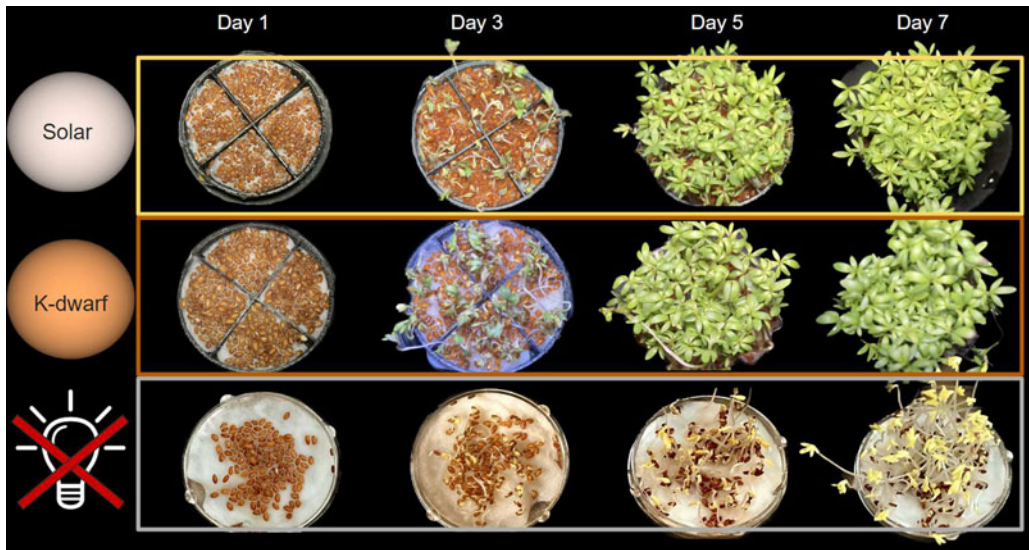


**Figure 1.** Garden cress (*Lepidium sativum*) grown on a sand substrate with one hundred initial seedlings under Solar (effective temperature 5800 K), K dwarf (effective temperature 4300 K) and dark conditions. Here the visual results for selected days are shown. Garden cress under K dwarf radiation sprouts sooner relative to Solar and dark conditions.

darkness grew the highest, but the seedlings that did sprout developed a ghostly white/yellow colour and grew leaves which folded onto themselves, rather than opening towards the light source like in the irradiated samples.

Figure 3(a) shows the incremental accumulation of dry mass of garden cress under Solar, K dwarf and dark conditions. The dry mass of garden cress has an increasing trend under Solar and K dwarf



**Figure 2.** Lateral perspective of garden cress (*Lepidium sativum*) grown under Solar, K dwarf and dark conditions on the seventh day after sowing.

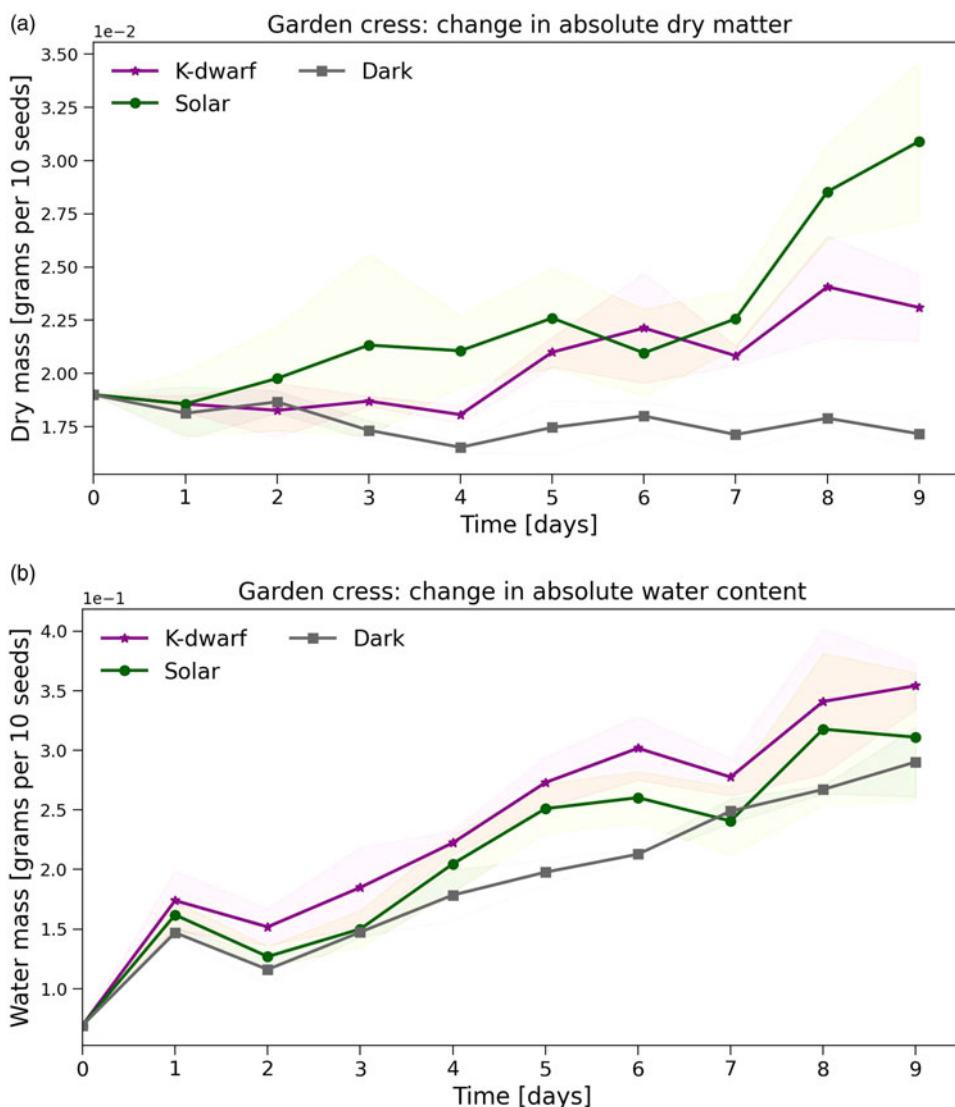


**Figure 3.** Dry mass accumulation and water absorption of garden cress under Solar, K dwarf and dark conditions with shaded standard deviations. (a) Dry mass accumulation of garden cress measured by desiccating the extracted material. (b) Absolute water contents of garden cress, calculated by subtracting the final dry masses from the initial fresh masses of the extracted material. The error bar is  $1\sigma$ .

radiation. Compared to this, garden cress under dark conditions fails to accumulate dry mass over time. In fact, its dry mass decreases with respect to initial values. Garden cress under Solar conditions exhibits slightly higher, but not significant, absolute dry masses compared to K dwarf conditions ( $p > 0.05$ , see Table S1). The absolute water contents of garden cress under the different radiation regimes are shown in Fig. 3(b). Garden cress under K dwarf light exhibits marginally higher, but not significant, water contents compared to Solar radiation ( $p > 0.05$ ; Table S1). Furthermore, garden cress under dark conditions, despite not accumulating any additional dry mass, does consistently absorb water throughout the entire experiment, albeit less than the illuminated plants.

The photosynthetic efficiencies of garden cress under Solar and K dwarf conditions on selected days can be seen in Fig. 4. The values for the dark scenario are omitted here, as the registered values were

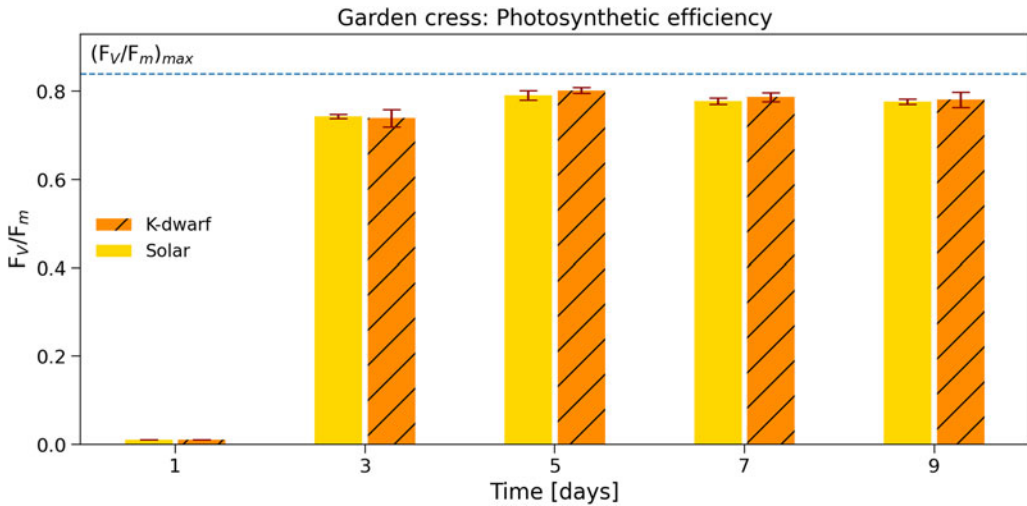


**Figure 4.** Photosynthetic efficiency of garden cress under Solar and K dwarf conditions on selected days measured with a pulse-amplitude-modulation fluorometer (PAM).  $F_m$  is the maximum fluorescence value and  $F_v$  is the difference between  $F_m$  and  $F_0$ , where  $F_0$  is the minimum fluorescence value. Plant  $F_v/F_m$  values range from 0.79 to 0.84, with smaller values indicating plant stress. The error bar is  $1\sigma$ .

due to photoconversion and not indicative of photosynthesis. The  $F_v/F_m$  values for the K dwarf scenario are comparable to those under Solar conditions (see Table 1). For example, on the last (ninth) day of the experiment, the  $F_v/F_m$  values are  $0.777 \pm 0.006$  and  $0.781 \pm 0.017$  for the Solar and K dwarf scenario, respectively. The differences in responses of the illuminated samples are not significant ( $p > 0.05$ , see Table S1).

**Table 1.** Photosynthetic efficiency values of garden cress (*Lepidium sativum*) and the cyanobacterium *Chroococcidiopsis* sp. CCME029 under solar and K dwarf radiation measured by a Pulse-Amplitude-Modulation fluorometer (mini-PAM).

Organism	Time [days]	K dwarf $[F_v/F_m \pm 1\sigma]$	Solar $[F_v/F_m \pm 1\sigma]$
Garden cress ( <i>Lepidium sativum</i> )	...	...	...
	3	$0.739 \pm 0.020$	$0.743 \pm 0.004$
	4	$0.797 \pm 0.010$	$0.788 \pm 0.021$
	5	$0.801 \pm 0.007$	$0.791 \pm 0.011$
	6	$0.797 \pm 0.009$	$0.805 \pm 0.008$
	7	$0.786 \pm 0.010$	$0.778 \pm 0.007$
	8	$0.780 \pm 0.022$	$0.778 \pm 0.008$
	9	$0.781 \pm 0.017$	$0.777 \pm 0.006$
	Cyanobacterium ( <i>Chroococcidiopsis</i> sp. CCME029)	...	...
7		$0.311 \pm 0.007$	$0.190 \pm 0.008$
10		<b><math>0.428 \pm 0.0</math></b>	$0.313 \pm 0.016$
12		<b><math>0.452 \pm 0.0</math></b>	$0.402 \pm 0.019$
13		<b><math>0.459 \pm 0.0</math></b>	$0.413 \pm 0.013$

Fluorescence parameters are as in Fig. 4. Fluorescence values for the cyanobacterium experiment are presented only from the seventh day onward, as prior to this time the culture spots are too diluted for reliable measurements. The standard deviation is  $1\sigma$ . For the K dwarf cyanobacterium sample, three out of four regions of interest (ROI; see Fig. 5) showed saturating fluorescence values from the tenth day of the experiment onward (see bold). As a result, these fluorescence values represent the lower limit of measurements and do not include a standard deviation.

**Cyanobacterium (*Chroococidiopsis sp. CCME 029*)**

Due to the growth patterns exhibited by this cyanobacterial strain, the experiment was extended for an additional period of four days compared to the garden cress experiments (Billi *et al.*, 2021). Figure 5(a) shows the phenotypes of the cyanobacterium cultures grown on Agar plates on the final day of the experiment under Solar, K dwarf and dark conditions. The cyanobacterium demonstrates a deepening of its green hue under both Solar and K dwarf conditions, whereas the cultures under constant dark conditions remained translucent with a light brown edge. Figure 5(b) shows the binary version of the images in panel (a). The pixel values within the regions of interest (ROI) under dark conditions are almost indistinguishable from the background pixels, whereas the pixels of the cultures under Solar and K dwarf radiation exhibit a clear edge and filled spots.

The photosynthetic efficiencies of the cyanobacterium from the seventh day of the experiment onward are shown in Table 1. Prior to this the culture spots are too diluted for reliable measurements. The photosynthetic efficiencies of the irradiated samples have an overall increasing trend. The maximum fluorescence signal of the K dwarf scenario with the initial pulse-amplitude-modulation fluorometer (PAM) settings was saturated for all but one spot from the tenth day of exposure onwards. This is why only the lower  $F_v/F_m$  limit was determined for this scenario (see Table 1). Overall, the cyanobacterium exhibited a significantly better response to K dwarf radiation in comparison to Solar radiation ( $p < 0.05$ , refer to Table S1).

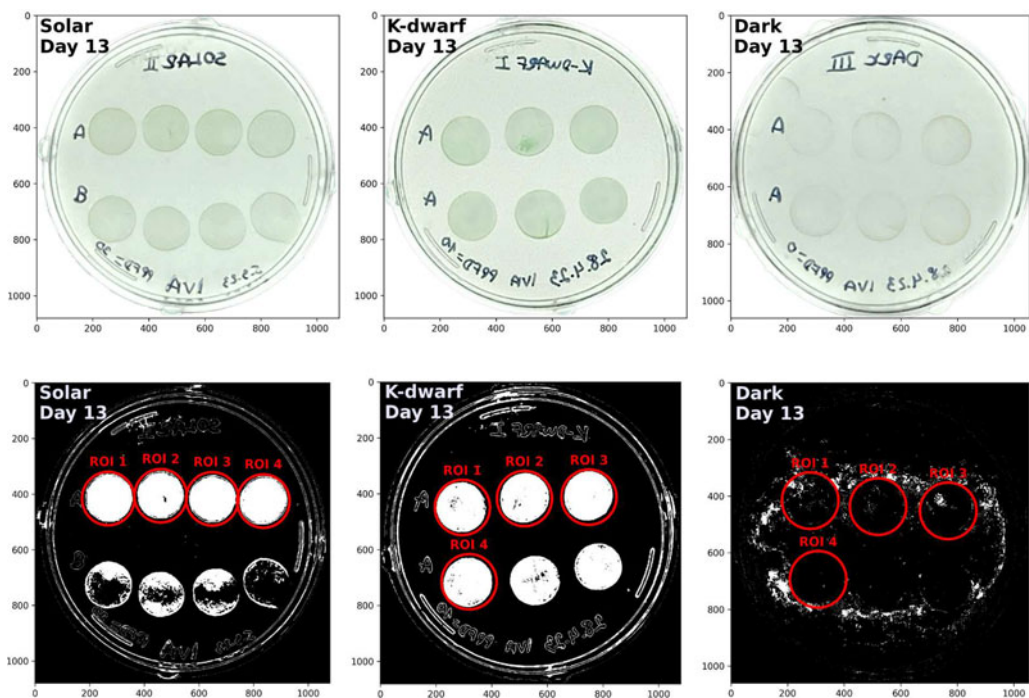


**Figure 5.** Cyanobacterium *Chroococidiopsis sp. CCME 029* on BG-11 Agar plate under Solar, K dwarf and dark conditions. (a) Day 13 after the start of the experiments. The drops correspond to an initial optical density of  $\sim 0.7$  at 730 nm. The Solar Agar plate contains row 'B,' which corresponds to an initial optical density of  $\sim 0.5$ , and which was not used in the analysis. (b) Binary version of the images in (a). White pixels have been selected through a colour threshold. The red circles depict the regions of interest (ROI), i.e. the drops for which the photosynthetic efficiencies and culture densities were determined.

The  $F_0$  incremental ratio, i.e.  $[F_0(\text{day } x) - F_0(\text{day } 0)] / F_0(\text{day } 0)$ , where  $x$  is the target day, is used as a measure of cyanobacterial culture growth (Perin *et al.*, 2015). Figure 6(a) shows the  $F_0$  incremental ratios for selected days under the Solar, K dwarf and dark regimes, which increase for the illuminated samples. The cyanobacterium under K dwarf conditions exhibits a significantly higher  $F_0$  incremental ratio with respect to Solar light ( $p < 0.05$ ; Table S1). Under continuous darkness, the cyanobacterium exhibits a decrease in  $F_0$  incremental ratios towards marginally negative values with time, as the cell concentration at the start of the experiment was higher than towards the end. Figure 6(b) shows the average integrated density (IntD) of the cyanobacterium which is an indicator of culture growth. The results show that the IntD increases with time for the illuminated samples, exhibiting overall higher, but not significant, values in the K dwarf compared to the Solar radiation regime ( $p > 0.05$ ). Cyanobacteria under constant dark conditions failed to exhibit significantly measurable IntD.

## Discussion

Understanding the effects of K dwarf radiation on photosynthesis and growth is of foremost importance not only for the assessment of its viability for phototrophic organisms but also for the interpretation of atmospheric biosignatures outside of the Solar System. However, there has been a dearth of experimental data on the responses of oxygenic photosynthetic organisms to simulated K dwarf light spectra. Most of the focus so far has been on cyanobacteria and plants exposed to the simulated radiation of the cooler counterparts, M dwarf stars (Claudi *et al.*, 2020; Battistuzzi *et al.*, 2023a, 2023b). In this study, to the best of our knowledge, we present the first experimental data on the responses of photosynthetic organisms to a simulated K dwarf spectrum.

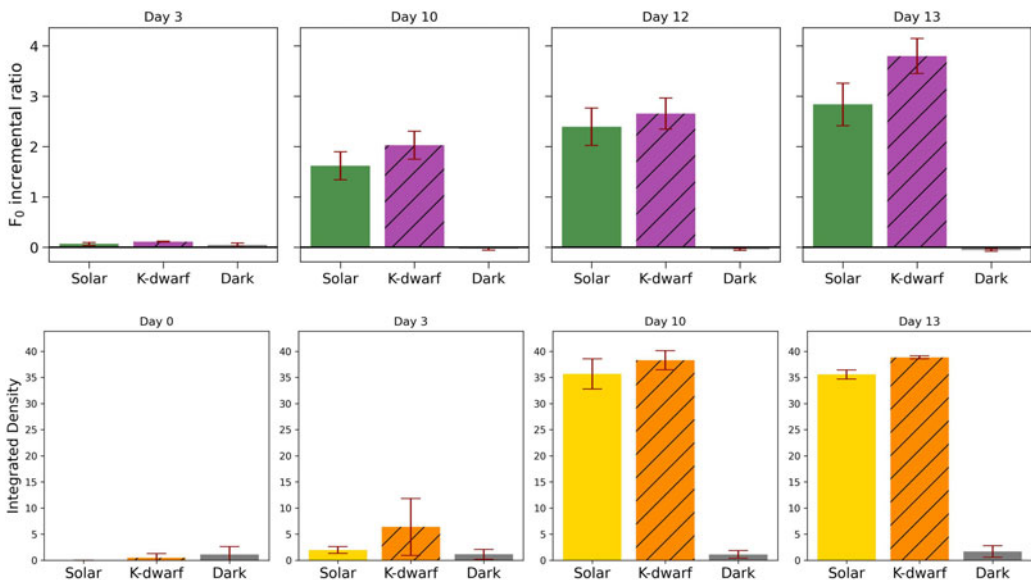


**Figure 6.**  $F_0$  incremental ratios and integrated densities of the cyanobacterium on selected days under Solar, K dwarf and dark conditions. (a)  $F_0$  incremental ratios ( $[F_0(\text{day } x) - F_0(\text{day } 0)] / F_0(\text{day } 0)$ ), where  $F_0$  is the minimum fluorescence value, are proportional to the increment of chlorophyll a, and thus, to the number of cells in the considered spot. As such it is used as an indicator of culture growth. The error bar is  $1\sigma$ . (b) Integrated densities, which were calculated in Python by summing up the raw values of all the pixels (RawIntD) within a region of interest (ROI) of an image (see e.g. Fig. 5) and multiplying it by the ratio of the image area in scaled units to the area in pixels:  $\text{IntD} = \text{RawIntD} \times (\text{Area in scaled units}) / (\text{Area in pixels})$ . As such, they are a measure of bacterial culture growth. The error bar is  $1\sigma$ .

It is important to keep in mind that the radiation intensities used for the garden cress experiments during the 12-h daytime period may not fully replicate the natural fluctuations in sunlight intensity experienced by plants in their native environment. Sunlight intensity on Earth varies throughout the day, with peak intensities occurring during the central hours. This variation is crucial for plants to adapt and respond to changing light conditions, including the activation of non-photochemical quenching (NPQ) to mitigate the effects of excess light. Our experimental design prioritizes controlled and reproducible conditions to investigate specific physiological responses under standardized environmental parameters, rather than the ideal growth conditions for a given organism. While our approach may not perfectly mirror real-world conditions, it allows us to isolate and study the effects of the two radiation regimes on plant physiology in a controlled setting. Previous studies have indicated that both shortwave and longwave radiation are necessary for the ideal growth of garden cress, which absorbs primarily in both the red (around 665–680 nm) and blue (around 430–450 nm) regions of the electromagnetic spectrum (Okamoto *et al.*, 1996; Ménard *et al.*, 2006; Guidi *et al.*, 2017; Ajdanian *et al.*, 2019). Our results, which demonstrate slightly higher dry masses for garden cress under Solar light, align with the biochemical parameters of the plant. This alignment is further supported by the fact that Solar light exhibits higher fluxes in the shortwave regime compared to K dwarf stars (see Fig. 7 in the Methods section). Furthermore, while we acknowledge the relationship between reduced

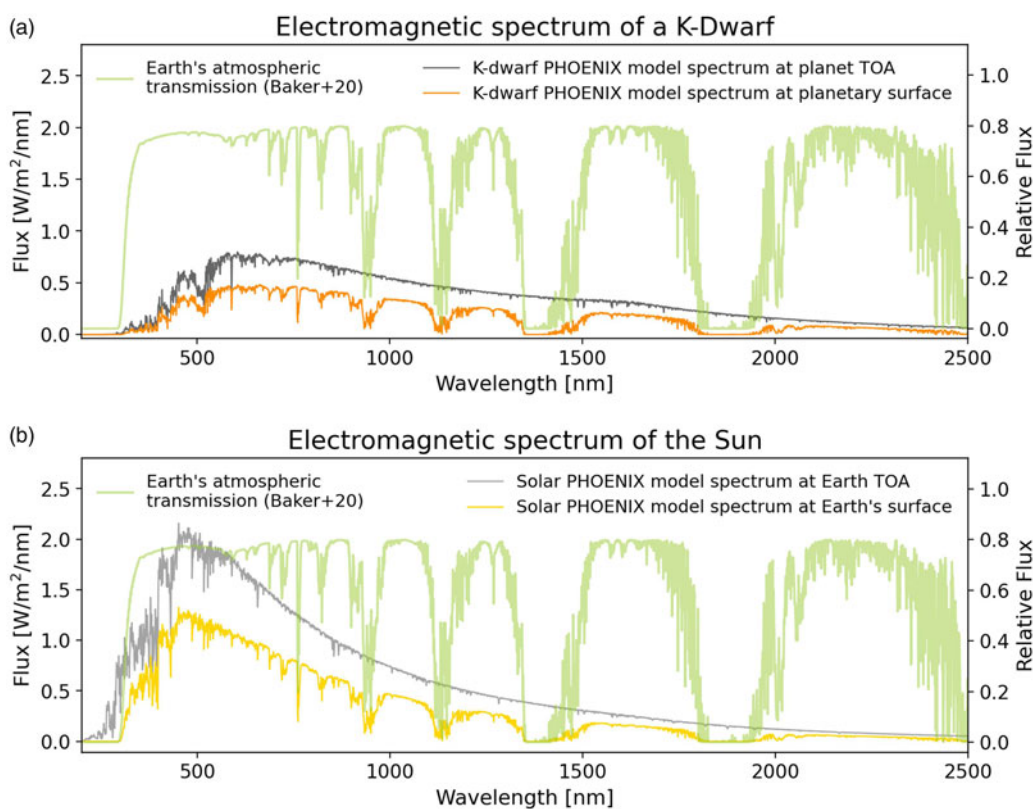


**Figure 7.** High-resolution spectra of the K dwarf star (upper panel) and the Sun (lower panel). The green spectrum in both panels is Earth's telluric (transmission) spectrum provided by Baker *et al.* (2020). Upper panel: the dark grey spectrum is the wavelength resolved top of the atmosphere (TOA) flux at  $\sim 0.441$  AU from the host star calculated in this work. The orange spectrum is the daily averaged model spectrum of a K dwarf star transmitted to the surface of our hypothetical planet with an Earth's telluric spectrum. The daily averaging was calculated by assuming a 12-h daylight cycle (see Methods). Lower panel: Same as in upper panel, but for the Earth/Sun system.

$F_v/F_m$  values and plant stress, it is worth highlighting that the differences observed between garden cress grown under Solar and K dwarf conditions are minor and not statistically significant (see Table 1 and Table S1 in the Supplementary Materials). Consequently, despite the association, these slight variances in  $F_v/F_m$  values do not conclusively indicate a substantial level of stress experienced by the garden cress under Solar radiation compared to K dwarf conditions.

Temperature measurements conducted throughout the experiments show stable conditions within the temperature ranges conducive to the growth of garden cress (Sattari Vayghan *et al.*, 2020) (see Fig. S3 in the Supplementary Materials). Despite small average temperature variations observed between experiments under the three radiation regimes, these variations do not substantially contribute to the differences in plant responses observed across the samples. Despite the differences in spectra, the plant showed the ability to grow similarly under K dwarf radiation compared to the Solar regime. This can be attributed to the adequate shortwave and increased longwave fluxes provided by the K dwarf spectrum. Notably, it exhibited this ability despite receiving three times lower photosynthetic photon flux densities (PPFD), which impact biomass accumulation and photosynthetic responses (see Fig. S1 and Table 2) (Welander and Ottosson, 1997; Ke *et al.*, 2021, 2023; Deo *et al.*, 2022). If garden cress, which has evolved under the light of our Sun, can demonstrate comparable growth when exposed to K dwarf radiation, it raises the possibility that garden cress evolved on an exoplanet orbiting a K dwarf star could potentially outperform Earth's garden cress in terms of biomass production. The cyanobacterium examined in this study has developed adaptations to endure various environmental stressors, including high radiation levels, and is commonly found in habitats with limited light availability, such as desert soils or endolithic environments (Friedmann, 1980; Billi *et al.*, 2017, 2019, 2021; Casero *et al.*, 2020). In such conditions, shorter-wavelength light is diminished due to scattering and absorption by the surrounding environment. Consequently, the cyanobacterium may have evolved to effectively utilize longer-wavelength light, which is less impacted by scattering and can penetrate deeper into microbial mats or substrates. Hence, considering that irradiation levels strongly fluctuate in desert environments, it is plausible that the light intensity used in this study for the K dwarf scenario falls within the range of natural irradiance variations and is thus preferred by the cyanobacterium.

**Table 2.** Summary of stellar and planetary parameters used in this work for the Sun–Earth and K dwarf–exoplanetary systems

	Earth/Sun	Exoplanet/K-star
Stellar type	G2 V	K4.5
Stellar effective temperature	5772 K	4285 K
Stellar mass	1 $M_{\odot}$	0.667 $M_{\odot}$
Stellar luminosity	1 $L_{\odot}$	0.116 $L_{\odot}$
Stellar radius	1 $R_{\odot}$	0.620 $R_{\odot}$
Star – planet distance	1 AU	0.441 AU
Effective flux at planetary top-of-atmosphere	1368 $W m^{-2}$ (= 1 · $S_0$ )	820.8 $W m^{-2}$ (= 0.6 · $S_0$ )
Effective flux at planetary surface	1115.4 $W m^{-2}$	621.2 $W m^{-2}$
Photosynthetic photon flux density (PPFD) for garden cress	1446 $\mu mol m^{-2} s^{-1}$	512 $\mu mol m^{-2} s^{-1}$
Photosynthetic photon flux density (PPFD) for cyanobacterium	30 $\mu mol m^{-2} s^{-1}$	10 $\mu mol m^{-2} s^{-1}$
Red to far-red photon flux ratio (R:FR)	1.28	1.16

The hypothetical exoplanet lies at 0.441 AU from its host K dwarf star, placing it in the centre of the habitable zone whose inner and outer boundary are given by the moist and maximum greenhouses, respectively. For a derivation of the values, see the Methods section and Supplementary Materials.  $S_0$  stands for the Solar constant.

These results can bring us closer to addressing which stellar environments could be the optimal candidates in the search for habitable worlds. We must keep in mind, though, that this study is constrained by the number and choice of organisms as well as by the evolutionary differences between them. For example, cyanobacteria evolved some 3.5 billion years ago, a time during which Earth received 0.75 times the Solar constant and the atmosphere contained orders of magnitude more carbon dioxide and less oxygen and ozone, causing the surface of the Earth to receive higher amounts of X-ray and UV radiation (Walker, 1985; Schopf and Packer, 1987; Kasting, 1993; Pavlov *et al.*, 2000; Cnossen *et al.*, 2007; Hessler, 2011; Kaltenegger *et al.*, 2020; Lehmer *et al.*, 2020; Payne *et al.*, 2020). This could have influenced the evolutionary trajectory of cyanobacteria, leading them to adapt to and favour lower-intensity and less energetic light. The K dwarf spectrum, with its reduced levels of radiation, may align better with the light conditions to which cyanobacteria were exposed during their evolutionary history. Garden cress, on the other hand, evolved much more recently, around the time when plants started transitioning from the oceans onto land some 400–300 million years ago (Dunn, 2013). This time was accompanied by a comparable Solar constant as well as oxygen, ozone and carbon dioxide levels to today (Glasspool and Scott, 2010; Dunn, 2013; Mills *et al.*, 2021). Garden cress, as a land plant, is influenced by a range of environmental cues that are intricately linked to Solar light and has evolved to thrive in such a terrestrial environment where it is exposed to more direct Solar light than the cyanobacterium. This can be seen in their photosynthetic pigments which evolved to absorb more shortwave light and is also consistent with the dry mass results under Solar irradiance of our study.

In addition to these experiments, the selection of a K dwarf as a host star is among several proposed factors that could enhance the potential habitability of an exoplanet (Heller and Armstrong, 2014; Arney, 2019; Schulze-Makuch *et al.*, 2020). Together with the right obliquity and eccentricity of a planet, these stars would provide the ‘goldilocks’ stellar environment for the emergence of superhabitable worlds and potential extraterrestrial life (Wolfe *et al.*, 2010; Cuntz and Guinan, 2016; Arney, 2019; Jernigan *et al.*, 2023). Hence, the results of this work are suggestive of the viability of photosynthesis that has evolved with a different parent star and can be used as a stepping stone to simulate signatures of oxygenic photosynthesis on exoplanets around K dwarf stars (Kiang *et al.*, 2007a, 2007b). This can aid in the interpretation of future exoplanetary atmospheric signatures obtained by e.g. JWST or studied by the KOBE or Terra Hunting experiments (Lillo-Box *et al.*, 2022; Naylor, *n.d.*).

## Conclusion

Garden cress exposed to K dwarf radiation shows comparable responses to those under Solar conditions, demonstrating the ability of the plant to grow under this alternative type of radiation. The cyanobacterium demonstrated a significantly more positive response to K dwarf radiation, exhibiting both higher photosynthetic activities and culture growth.

These findings not only highlight the coping mechanisms of photosynthetic organisms to modified radiation environments but also they imply the principal habitability of exoplanets orbiting K dwarf stars. Understanding the responses of organisms to different spectra is not only crucial for assessing the suitability of K dwarfs as host stars for habitable exoplanets but also for interpreting atmospheric biosignatures beyond our Solar System. To obtain a holistic understanding of the responses to K dwarf radiation, further investigations should focus on the choice of representative organisms from Earth’s major biomes, such as aquatic ecosystems, grasslands, forests, deserts and tundra. Beyond the choice of biological organisms, these experiments could further be enhanced by incorporating an environmental simulation chamber which would allow modification and monitoring of ambient gases, pressures and temperatures. Additionally, variations in day length as well as a simulated twilight period could be introduced to make the experiments more realistic. The results of these future experiments could make this study a benchmark on a long road of laboratory tests that can be used to prioritize extrasolar planets for costly follow-up observations like transit spectroscopy.

## Methods

### General experimental course

In this work we conducted experiments to evaluate the viability of K dwarf radiation on photosynthetic organisms using a starlight simulator. The subsequent outline constituted the entirety of the experiments:

- I. To simulate the stellar spectra, we used an LED stellar simulator with a variable spectrum module which allows for the reproduction of a variety of spectral environments in the 350–1500 nm wavelength range.
- II. We modelled the emission spectrum of a ~4300 Kelvin K dwarf star (i.e. spectral type: K4.5) using the PHOENIX spectral library (Husser *et al.*, 2013). We calculated the daily globally averaged electromagnetic spectrum of the K dwarf star transmitted to the surface of a hypothetical planet with an Earth-like atmosphere in the centre of its habitable zone (Kopparapu *et al.*, 2013). We repeated the calculations for the Sun to obtain the control radiation. Both spectra were used as an input for the LED stellar simulator.
- III. Given the rationale that Earth-like planets in the centres of the habitable zones of most K dwarf stars (i.e. with masses higher than ~0.5 solar masses) lie outside of the radius at which a planet in a circular orbit would be tidally locked (Kasting *et al.*, 1993), we introduce a 12-h day night cycle in all of the experiments in the form of a square wave.
- IV. We built a small external light isolating chamber in which the selected photosynthetic organisms were hosted during the experiments. Ambient conditions were logged with a temperature and humidity sensor.
- V. Samples of the selected photosynthetic organisms were subsequently exposed to solar, K dwarf as well as continuously dark conditions for 9 and 13 days (for garden cress and cyanobacterium experiments, respectively) and their responses were determined in post-experimental analysis.

### Model spectra

#### Calculating the modelled K dwarf spectrum at the planetary surface

We calculated the wavelength resolved flux received at the surface of the K dwarf planet by multiplying the wavelength resolved top-of-the-atmosphere (TOA) flux with the transmission (telluric) spectrum of Earth provided to us by Baker *et al.* (2020). Their code wraps the *Planetary Spectrum Generator* (PSG) radiative transfer tool to calculate the Earth spectra and has a lower limit at 200 nm (Villanueva *et al.*, 2018). This transmission spectrum was calculated at zenith over Göttingen, Germany on a random fall day and reveals the composition of Earth's atmosphere, with its prominent water vapour absorption bands (see Fig. 7). The transmission spectrum of Earth serves as a first proxy towards assessing surface conditions of potentially habitable exoplanets. To the best of our knowledge, we calculated for the first time the stellar spectrum of a K dwarf star transmitted to the surface of a hypothetical habitable zone planet with an Earth-like atmosphere using Earth's telluric spectrum (see upper panel of Fig. 7). Analogously, we modelled the emission spectrum of the Sun using the PHOENIX spectral library and placed the Earth at 1 AU, where it receives one Solar constant  $S_0$ . We calculated the emission spectrum at TOA as well as the Solar daily averaged spectrum transmitted to the surface of Earth using Earth's telluric spectrum (see lower panel of Fig. 7). A numerical summary for the Earth–Sun and Exoplanet–K dwarf systems is presented in Table 2.

#### Creating the starlight simulator

For the starlight simulator we used the Pico LED small area Solar simulator with the *Variable Spectra Module* (VSM) from the manufacturer *G2V Optics Inc.* The VSM allows for software-controlled intensity manipulation of up to 30 LED channels, which are treated as linear superpositions of up to three

skew Gaussian functions, in the wavelength range 350–1500 nm, to replicate a variety of Solar as well as other stellar conditions.

We produced a nonlinear fit to the modelled PHOENIX surface spectra which we used as input to communicate with the individual LED channels of the *Pico* software (see ‘simulated’ spectra in Fig. 8). We used *Python* to visualize the produced fits in comparison to our modelled spectra and manually further tweaked the fits to minimize the discrepancies. The final *Pico* fits (i.e. ‘simulated spectra’) and the corresponding modelled surface spectra are shown in Fig. 8. An automatic day/night cycle (i.e. 12-h cyclical switching on and off the lamp) was also implemented in *Python* in the form of a square wave to ensure a more consistent experimental progression.

### Laboratory procedures

#### Garden cress: dry matter accumulation and water intake

Garden cress seeds (*Lepidium sativum*) were exposed to simulated Solar and K dwarf radiation and the dry and fresh masses of the seedlings were measured to determine the changes in biomass through time. The garden cress is a rapidly growing annual herb which is adaptable to diverse climates and soil conditions, and as such makes an excellent astrobiological target (Nehdi *et al.*, 2012; Wadhwa *et al.*, 2012). The experiment was also run under dark conditions to ensure that the relative growth of garden cress under K dwarf and solar conditions is in fact due to radiation and not due to the intrinsic availability of nutrients in the plant seeds themselves. The irradiated samples were positioned at a stand at 3 cm to the base of the setup, equalling 8 cm to the irradiation source. Sand was used as the substrate as it allowed for the complete daily extraction of the sample, i.e. of the sprouted seedlings and the entirety of their roots. The methodology of measuring the fresh and dry mass of the sample is based on several works for measuring biomass accumulation (‘Dry mass change during germination of bean seeds’, n.d.; Hoh, 2002; Filson, 2005). Four independent biological replicates of garden cress were used for the experiments.

The following steps were implemented:

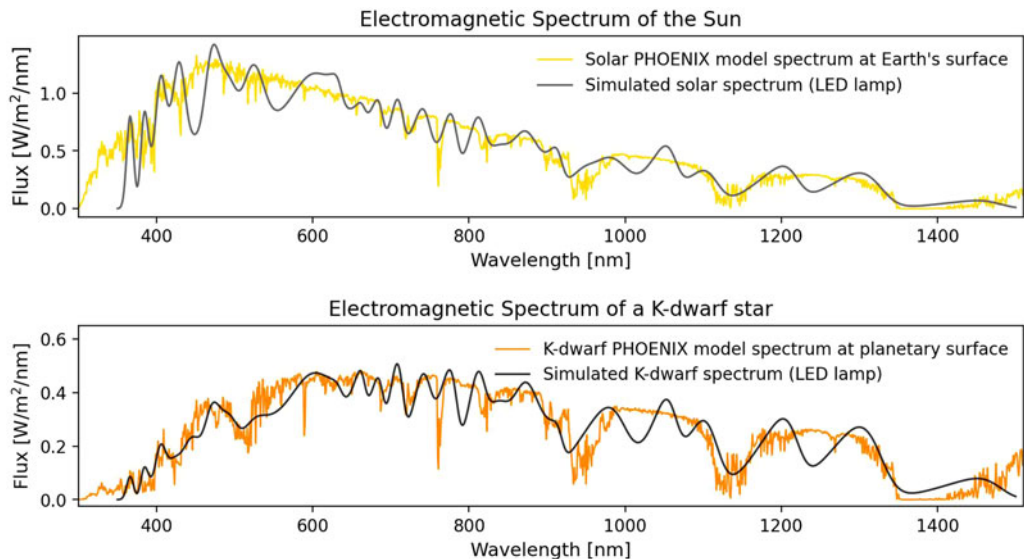


**Figure 8.** Modelled surface spectra from Fig. 7 and their corresponding LED lamp simulations. The lamp has 30 tunable LED channels which are treated as linear superpositions of up to three skew Gaussian functions whose intensities can be manipulated individually. The simulated spectra are used as input to communicate with the LED software.

**1) Control group:**

A sample of 90 control garden cress seeds was used.

- a) The fresh masses of nine groups à la ten control seeds were measured on a digital  $1.0 \times 10^{-4}$  g precision scale. The mean and standard deviation for the nine groups of ten control seeds was calculated.
- b) The nine groups à la ten seeds were desiccated by drying in an oven at  $40^{\circ}\text{C}$  for two to three days and subsequently in a vacuum desiccator until a constant dry mass was reached. This was the case after a further two to three days.
- c) The final dry masses of nine groups à la ten control seeds were measured, and the mean and standard deviation were calculated once more.

**2) Experimental group:**

A further sample of 90 experimental garden cress seeds was used. The following steps were performed for the Solar and K dwarf radiation sources implementing a 12-h day night cycle, as well as for dark conditions.

*Pre-experiment*

- a) The fresh masses of nine groups à la 9 experimental group garden cress seeds were measured on the digital  $1.0 \times 10^{-4}$  g precision scale. The mean and standard deviation for the 9 groups of 10 control seeds was calculated.
- b) Those 90 seeds were soaked and rinsed with tap water.
- c) A sand substrate was placed in a 5 cm-diameter Petri dish and wetted with water.
- d) The ninety rinsed seeds were initially placed on the wet sand using laboratory tweezers and then placed under the radiation (or in a closed  $40 \times 40 \times 20$  cm box for the dark scenario).

*During experiment*

- e) Temperatures and relative humidity levels were tracked and logged with a temperature- and humidity sensor throughout the full duration of the experiment (see Fig. S3 in the Supplementary Materials).
- f) The plants were watered daily with a constant amount of water, ensuring consistent hydration levels throughout the duration of the experiments.
- g) A random selection of 10 seeds, including roots, was extracted from the population every 24 h for a total of 9 days – the interval between consecutive measures remained equal for consistency.
- h) The extracted seeds/seedlings/plant matter were thoroughly rinsed to remove sand remnants.

*Post-experiment*

- i) The fresh masses of the extracted material were measured on the digital  $1.0 \times 10^{-4}$  g precision scale every 24 h.
- j) The extracted material was desiccated until a constant mass was reached, including 2–3 days in the oven at  $40^{\circ}\text{C}$  and a further 2–3 days in the vacuum desiccator.
- k) The final dry masses of the extracted seeds/seedlings/plant matter were measured.

Although the experiments conducted under different radiation regimes share the confounding variable of seed proximity, potentially resulting in shading and altered growth patterns due to the rapid germination of the first seeds (Casal, 2013), the random selection of seedlings for analysis in both scenarios facilitates a comparative evaluation of the plant's reaction to the modified light conditions. While acknowledging the potential influence of seed proximity on plant growth, the random sampling approach helps mitigate any systematic biases associated with this shared variable. Consequently, we contend that the observed differences in plant responses predominantly reflect the effects of the varying light conditions.

*Garden cress: photosynthetic efficiency*

The photosynthetic efficiency of garden cress under Solar-, K dwarf and dark conditions was measured with the Mini-PAM II (Pulse-Amplitude-Modulation, Walz, Germany) fluorometer which determined chlorophyll *a* (Chl *a*) fluorescence yields. Chl *a* fluorescence yields serve as an indicator for photosynthetic performance and are often used to identify chemical or environmental stressors (Ogren, 1990; Percival and Sheriffs, 2002; Percival, 2005). In this work, the fibre optics tip of the Mini-PAM was placed at 2 cm to sample level and was aligned at a 60° angle relative to the measuring plane with a 1 cm-diameter measuring area. The maximum photochemical quantum yield ( $F_v/F_m$ ) of the photosystem II (PSII) is given by the equation:  $F_v/F_m = (F_m - F_0) / F_m$ , where  $F_m$  is the maximum fluorescence level in mV generated by a 0.6 s saturation pulse (SP) which closes all PSII reaction centres and  $F_0$  is the minimum fluorescence level in mV excited by a very low-intensity measuring light (ML; frequency = 5 Hz) to keep PSII reaction centres open (Kitajima and Butler, 1975; Genty *et al.*, 1989). A ML intensity setting of 12 corresponds to  $6000 \mu\text{mol m}^{-2} \text{s}^{-1}$  at a 7 mm fibre-optics-to-sample-level distance and is adjusted at increments of  $500 \mu\text{mol m}^{-2} \text{s}^{-1}$ . The final PAM settings can be found in Fig. S2.  $F_v/F_m$  was measured on a sample which had been acclimated to the dark for 25–30 min.

To ensure a denser plant population and a more uniform surface area, we conducted the photosynthetic efficiency experiments by sprinkling a handful of garden cress seeds onto a sterile cotton substrate. We opted for sterile cotton as the substrate because the weight and adhesive properties of wetted sand grains would have hindered the growth of the cress seeds. All measurements under the PAM settings were obtained from four independent biological replicates of garden cress under Solar, K dwarf and dark conditions. The parameter values were measured every 24 h for 9 days per illumination-type and biological replica.

*Cyanobacteria: photosynthetic efficiency and integrated density*

We used the desert cyanobacterium *Chroococidiopsis* sp. CCMEE 029 (Culture Collection of Microorganisms from Extreme Environments) extracted from the Negev Desert in Israel for this portion of the study. Cyanobacteria are believed to contribute to 20–30% of the Earth's primary photosynthetic productivity and have a collective worldwide biomass of approximately  $3 \times 10^{14}$  grams of carbon (Garcia-Pichel *et al.*, 2003; Pisciotta *et al.*, 2010). As such, this strain makes an excellent astrobiological target which can withstand a variety of extreme conditions and can be found in numerous environments (Cumbers and Rothschild, 2014; Billi *et al.*, 2017, 2019). We grew the cyanobacterium culture in a liquid BG-11 medium with a  $10^{-1}$  dilution in a 25°C incubator without shaking under a 4000 Kelvin cold LED lamp until it reached an exponential growth phase. At this point we transferred the culture to a BG-11 Agar plate in 20 microliter-sized drops. Given that this cyanobacterial strain exhibits an optimal growth at intensities much smaller than garden cress, i.e. PAR intensities of 30–40  $\mu\text{mol}$  (photons)  $\text{m}^{-2} \text{s}^{-1}$ , we decreased the wavelength-distributed flux of the modelled Solar emission spectrum as well as its corresponding simulated LED spectrum by 48 times. The PPFD used for the Solar sample was therefore 30  $\mu\text{mol}$  (photons)  $\text{m}^{-2} \text{s}^{-1}$ . To keep the original photonal ratio of the two spectral types, the K dwarf PAR intensity was decreased to 10  $\mu\text{mol}$  (photons)  $\text{m}^{-2} \text{s}^{-1}$  (see Table 2). We then exposed the Agar plate to these radiation regimes for 13 days, implementing a 12-h day night cycle. Every few days we documented the visual changes of the culture with a camera. Four independent biological replicates of the cyanobacterial strain were used for the experiments.

We measured the photosynthetic efficiencies of dark-acclimated samples with the mini-PAM fluorometer. We used Gain level 3 and a ML intensity of 12 in the PAM settings to capture the low photosynthetic signal of the cyanobacterium spots in the initial phases of the experiments. The remaining settings were as for the garden cress experiments (see Fig. S2). We calculated the corresponding integrated densities (IntD) with *Python* by summing up the raw values of all the pixels (RawIntD) within a region of interest (ROI) in the image (see e.g. Fig. 5 in the main text) and multiplying it by the ratio of the image area in scaled units to the area in pixels:

$$\text{IntD} = \text{RawIntD} \times (\text{Area in scaled units}) / (\text{Area in pixels}) \quad (1)$$

We used an RGB (red, green and blue) pixel range of  $\pm 10$  around the average RGB values of all regions of interest as a colour threshold and calculated the integrated densities of each spot. The threshold captures all tonalities of pixels in the samples in accordance with their contribution to the culture growth.

**Supplementary material.** The supplementary material for this article can be found at <https://doi.org/10.1017/S1473550424000132>.

**Data availability.** All data generated or analyzed during this study are included in this published article and their sources are cited where applicable. Correspondence and requests for materials should be addressed to Iva Vilović.

**Acknowledgements.** The first author would like to thank the scholarship organization *Studienstiftung des deutschen Volkes* without which this work would not have been possible. The authors also thank professor Dr Bernd Szyszka and his Ph.D. student Sri Hari Bharath Vinoth Kumar at the Technische Universität Berlin for providing the essential *Pico* LED small area solar simulator from the manufacturer *G2V Optics Inc.* for the experiments. The authors also thank Dr Ashley D. Baker for providing us with the invaluable telluric spectrum of Earth. Furthermore, the authors thank Dr Nicoletta La Rocca and her research group at the University of Padova for invaluable input and advice concerning the experimental setup of the cyanobacterial portion of this work.

**Financial support.** *Studienstiftung des deutschen Volkes* doctoral scholarship (IV), PLATO Data Center grant 50001501 (RH).

**Author contributions.** Conceptualization: DSM. Methodology: IV, DSM, RH. Investigation: IV. Visualization: IV. Formal analysis: IV, RH. Funding acquisition: IV. Supervision: DSM, RH. Writing – original draft: IV.

**Competing interest.** None.

## References

- Adams FC, Bodenheimer P and Laughlin G (2005) M dwarfs: planet formation and long term evolution. *Astronomische Nachrichten* **326**, 913–919.
- Ajdanian L, Babaei M and Aroee H (2019) The growth and development of cress (*Lepidium sativum*) affected by blue and red light. *Helicon* **5**, e02109.
- Anglada-Escudé G, Amado PJ, Barnes J, Berdiñas ZM, Butler RP, Coleman GAL, de la Cueva I, Dreizler S, Endl M, Giesers B, Jeffers SV, Jenkins JS, Jones HRA, Kiraga M, Kürster M, López-González MJ, Marvin CJ, Morales N, Morin J, Nelson RP, Ortiz JL, Ofir A, Paardekooper S-J, Reiners A, Rodríguez E, Rodríguez-López C, Sarmiento LF, Strachan JP, Tsapras Y, Tuomi M and Zechmeister M (2016) A terrestrial planet candidate in a temperate orbit around Proxima Centauri. *Nature* **536**, 437–440.
- Arney GN (2019) The K dwarf advantage for biosignatures on directly imaged exoplanets. *Astrophysical Journal Letters* **873**, L7.
- Baker AD, Blake CH and Reiners A (2020) The IAG solar flux atlas: telluric correction with a semiempirical model. *Astrophysical Journal Supplement Series* **247**, 24.
- Barnes R (2017) Tidal locking of habitable exoplanets. *Celestial Mechanics and Dynamical Astronomy* **129**, 509–536.
- Barnes R, Jackson B, Greenberg R and Raymond SN (2009) Tidal limits to planetary habitability. *Astrophysical Journal* **700**, L30–L33.
- Battistuzzi M, Cocola L, Claudi R, Pozzer AC, Segalla A, Simionato D, Morosinotto T, Poletto L and La Rocca N (2023a) Oxygenic photosynthetic responses of cyanobacteria exposed under an M-dwarf starlight simulator: implications for exoplanet's habitability. *Frontiers in Plant Science* **14**, 1070359.
- Battistuzzi M, Cocola L, Liistro E, Claudi R, Poletto L and La Rocca N (2023b) Growth and photosynthetic efficiency of microalgae and plants with different levels of complexity exposed to a simulated M-dwarf starlight. *Life* **13**(8), 1641. <https://doi.org/10.3390/life13081641>
- Battistuzzi M, Morlino MS, Cocola L, Trainotti L, Treu L, Campanaro S, Claudi R, Poletto L and La Rocca N (2023c) Transcriptomic and photosynthetic analyses of *Synechocystis* sp. PCC6803 and *Chlorogloeopsis fritschii* sp. PCC6912 exposed to an M-dwarf spectrum under an anoxic atmosphere. *Front. Plant Science* **14**, 1322052.
- Billi D, Baqué M, Verseux C, Rothschild L and de Vera J-P (2017) Desert cyanobacteria: potential for space and earth applications. In Stan-Lotter H and Fendrihan S (eds), *Adaption of Microbial Life to Environmental Extremes: Novel Research Results and Application*. Cham: Springer International Publishing, pp. 133–146. [https://doi.org/10.1007/978-3-319-48327-6\\_6](https://doi.org/10.1007/978-3-319-48327-6_6).
- Billi D, Staibano C, Verseux C, Fagliarone C, Mosca C, Baqué M, Rabbow E and Rettberg P (2019) Dried biofilms of desert strains of *Chroococcidiopsis* survived prolonged exposure to space and Mars-like conditions in low Earth orbit. *Astrobiology* **19**, 1008–1017.
- Billi D, Fernandez BG, Fagliarone C, Chiavarini S and Rothschild LJ (2021) Exploiting a perchlorate-tolerant desert cyanobacterium to support bacterial growth for *in situ* resource utilization on Mars. *International Journal of Astrobiology* **20**, 29–35.
- Casal JJ (2013) Photoreceptor signaling networks in plant responses to shade. *Annual Review of Plant Biology* **64**, 403–427.
- Casero MC, Ascaso C, Quesada A, Mazur-Marzec H and Wierchos J (2020) Response of endolithic *Chroococcidiopsis* strains from the polyextreme Atacama desert to light radiation. *Frontiers in Microbiology* **11**, 614875.
- Claudi R, Alei E, Battistuzzi M, Cocola L, Erculiani MS, Pozzer AC, Salasnich B, Simionato D, Squicciarini V, Poletto L and La Rocca N (2020) Super-Earths, M dwarfs, and photosynthetic organisms: habitability in the lab. *Life* **11**(1), 10. <https://doi.org/10.3390/life11010010>

- Crossen I, Sanz-Forcada J, Favata F, Witasse O, Zegers T and Arnold NF (2007) Habitat of early life: solar X-ray and UV radiation at Earth's surface 4–3.5 billion years ago. *Journal of Geophysical Research: Planets* **112**(E2). <https://doi.org/10.1029/2006je002784>
- Cumbers J and Rothschild LJ (2014) Salt tolerance and polyphyly in the cyanobacterium *Chroococcidiopsis* (Pleurocapsales). *Journal of Phycology* **50**, 472–482.
- Cuntz M and Guinan EF (2016) About exobiology: the case for dwarf L stars. *Astrophysical Journal* **827**, 79.
- Deo RC, Grant RH, Webb A, Ghimire S, Igoe DP, Downs NJ, Al-Musaylh MS, Parisi AV and Soar J (2022) Forecasting solar photosynthetic photon flux density under cloud cover effects: novel predictive model using convolutional neural network integrated with long short-term memory network. *Stochastic Environmental Research and Risk Assessment* **36**, 3183–3220.
- Dole SH and Henry HF (1966) Book reviews: habitable planets for man. *Physics Teacher* **4**, 138–142.
- Dry mass change during germination of bean seeds [WWW Document] (n.d.) StudyCorgi.com. Available at <https://studycorgi.com/dry-mass-change-during-germination-of-bean-seeds/> (Accessed 12 July 2022).
- Dunn CW (2013) Evolution: out of the ocean. *Current Biology* **23**(4), R143–R145. <https://doi.org/10.1016/j.cub.2013.01.067>
- Filson GC (ed.) (2005) *Intensive Agriculture and Sustainability: A Farming Systems Analysis*, 1st edn. Vancouver: UBC Press.
- Friedmann EI (1980) Endolithic microbial life in hot and cold deserts. *Origins of Life* **10**, 223–235.
- García-Pichel F, Belnap J, Neuer S and Schanz F (2003) Estimates of global cyanobacterial biomass and its distribution. *Archiv für Hydrobiologie – Supplement: Algological Studies* **109**, 213.
- Gebauer S, Vilović I, Grenfell JL, Wunderlich F, Schreier F and Rauer H (2021) Influence of biomass emissions on habitability, biosignatures, and detectability in Earth-like atmospheres. *ApJ* **909**, 128.
- Genty B, Briantais J-M and Baker NR (1989) The relationship between the quantum yield of photosynthetic electron transport and quenching of chlorophyll fluorescence. *Biochimica et Biophysica Acta (BBA) – General Subjects* **990**, 87–92.
- Gillon M, Jehin E, Lederer SM, Delrez L, de Wit J, Burdanov A, Van Grootel V, Burgasser AJ, Triaud AHMJ, Opitom C, Demory B-O, Sahu DK, Bardalez Gagliuffi D, Magain P and Queloz D (2016) Temperate Earth-sized planets transiting a nearby ultracool dwarf star. *Nature* **533**, 221–224.
- Gillon M, Triaud AHMJ, Demory B-O, Jehin E, Agol E, Deck KM, Lederer SM, de Wit J, Burdanov A, Ingalls JG, Bolmont E, Lecante J, Raymond SN, Selsis F, Turbet M, Barkaoui K, Burgasser A, Burleigh MR, Carey SJ, Chaushev A, Copperwheat CM, Delrez L, Fernandes CS, Holdsworth DL, Kotze EJ, Van Grootel V, Almlaeky Y, Benkhaldoun Z, Magain P and Queloz D (2017) Seven temperate terrestrial planets around the nearby ultracool dwarf star TRAPPIST-1. *Nature* **542**, 456–460.
- Glasspool IJ and Scott AC (2010) Phanerozoic concentrations of atmospheric oxygen reconstructed from sedimentary charcoal. *Nature Geoscience* **3**, 627–630.
- Guidi L, Tattini M, Landi M, Agati G, Fini A, Ferrini F, Gori A, Pardossi A (2017) How does chloroplast protect chlorophyll against excessive light. *Chlorophyll* **21**, 21–36.
- Heller R and Armstrong J (2014) Superhabitable worlds. *Astrobiology* **14**(1), 50–66. <https://doi.org/10.1089/ast.2013.1088>
- Heller R, Leconte J and Barnes R (2011) Tidal obliquity evolution of potentially habitable planets. *Astronomy & Astrophysics* **528**, A27.
- Hessler AM (2011) Earth's Earliest Climate. *Nature Education Knowledge* **3**(10), 24. Available at: <https://www.nature.com/scitable/knowledge/library/earth-s-earliest-climate-24206248/> (Accessed 15 July 2023)
- Hoh YK (2002) *Longman A-Level Biology: Growth, Development and Reproduction*. Singapore: Pearson Education South Asia.
- Husser T-O, Wende-von Berg S, Dreizler S, Homeier D, Reiners A, Barman T and Hauschildt PH (2013) A new extensive library of PHOENIX stellar atmospheres and synthetic spectra. *Astronomy and Astrophysics Supplement Series* **553**, A6.
- Jernigan J, Lafèche É, Burke A and Olson S (2023) Superhabitability of high-obliquity and high-eccentricity planets. *Astrophysical Journal* **944**, 205.
- Kaltenegger L, Lin Z and Madden J (2020) High-resolution transmission spectra of Earth through geological time. *Astrophysical Journal Letters* **892**, L17.
- Kasting JF (1993) Earth's early atmosphere. *Science* **259**, 920–926.
- Kasting JF, Whitmire DP and Reynolds RT (1993) Habitable zones around main sequence stars. *Icarus* **101**, 108–128.
- Ke X, Yoshida H, Hikosaka S and Goto E (2021) Optimization of photosynthetic photon flux density and light quality for increasing radiation-use efficiency in dwarf tomato under LED light at the vegetative growth stage. *Plants* **11**, 121.
- Ke X, Yoshida H, Hikosaka S and Goto E (2023) Photosynthetic photon flux density affects fruit biomass radiation-use efficiency of dwarf tomatoes under LED light at the reproductive growth stage. *Frontiers in Plant Science* **14**, 1076423.
- Kiang NY, Segura A, Tinetti G, Govindjee, Blankenship RE, Cohen M, Siefert J, Crisp D and Meadows VS (2007a) Spectral signatures of photosynthesis. II. Coevolution with other stars and the atmosphere on extrasolar worlds. *Astrobiology* **7**, 252–274.
- Kiang NY, Siefert J, Govindjee, Blankenship RE (2007b) Spectral signatures of photosynthesis. I. Review of Earth organisms. *Astrobiology* **7**, 222–251.
- Kitajima M and Butler WL (1975) Quenching of chlorophyll fluorescence and primary photochemistry in chloroplasts by dibromothymoquinone. *Biochimica et Biophysica Acta* **376**, 105–115.
- Kopparapu RK, Ramirez R, Kasting JF, Eymet V, Robinson TD, Mahadevan S, Terrien RC, Domagal-Goldman S, Meadows V and Deshpande R (2013) Habitable zones around main-sequence stars: new estimates. *Astrophysical Journal* **765**, 131.
- Lehmer OR, Catling DC, Buick R, Brownlee DE and Newport S (2020) Atmospheric CO<sub>2</sub> levels from 2.7 billion years ago inferred from micrometeorite oxidation. *Science Advances* **6**, eaay4644.
- Lillo-Box J, Santos NC, Santerne A, Silva AM, Barrado D, Faria J, Castro-González A, Balsalobre-Ruza O, Morales-Calderón M, Saavedra A, Marfil E, Sousa SG, Adibekyan V, Berihuete A, Barros SCC, Delgado-Mena E, Huéllamo N, Deleuil M,

- Demangeon ODS, Figueira P, Grouffal S, Aceituno J, Azzaro M, Bergond G, Fernández-Martín A, Galadí D, Gallego E, Gardini A, Góngora S, Guijarro A, Hermelo I, Martín P, Mínguez P, Montoya LM, Pedraz S and Vico Linares JI (2022) The KOBE experiment: K-dwarfs orbited by habitable exoplanets – project goals, target selection, and stellar characterization. *Astronomy and Astrophysics Supplement Series* **667**, A102.
- Luger R and Barnes R (2015) Extreme water loss and abiotic O<sub>2</sub> buildup on planets throughout the habitable zones of M dwarfs. *Astrobiology* **15**, 119–143.
- Ménard C, Dorais M, Hovi T and Gosselin A (2006) Developmental and physiological responses of tomato and cucumber to additional blue light. *Acta Horticulturae* **711**, 291–296. <https://doi.org/10.17660/actahortic.2006.711.39>
- Mills BJW, Donnadieu Y and Goddérís Y (2021) Spatial continuous integration of Phanerozoic global biogeochemistry and climate. *Gondwana Research* **100**, 73–86.
- Naylor T (n.d.) Terra Hunting Experiment [WWW Document]. Available at <https://www.terrahunting.org/about.html> (Accessed 27 June 2023).
- Nehdi IA, Sbihi H, Tan CP and Al-Resayes SI (2012) Garden cress (*Lepidium sativum* Linn.) seed oil as a potential feedstock for biodiesel production. *Bioresource Technology* **126**, 193–197.
- Ogren E (1990) Evaluation of chlorophyll fluorescence as a probe for drought stress in willow leaves. *Plant Physiology* **93**, 1280–1285.
- Okamoto K, Yanagi T, Takita S, Tanaka M, Higuchi T, Ushida Y and Watanabe H (1996) Development of plant growth apparatus using blue and red LED as artificial light source. *Acta Horticulturae* **440**, 111–116.
- Pavlov AA, Kasting JF, Brown LL, Rages KA and Freedman R (2000) Greenhouse warming by CH<sub>4</sub> in the atmosphere of early Earth. *Journal of Geophysical Research* **105**, 11981–11990.
- Payne RC, Brownlee D and Kasting JF (2020) Oxidized micrometeorites suggest either high pCO<sub>2</sub> or low pN<sub>2</sub> during the Neoproterozoic. *Proceedings of the National Academy of Sciences of the United States of America* **117**, 13660–13666.
- Peale SJ (1977) *Rotation Histories of the Natural Satellites, IAU Colloq. 28: Planetary Satellites*. Tucson: University of Arizona Press, pp. 87–112.
- Percival GC (2005) The use of chlorophyll fluorescence to identify chemical and environmental stress in leaf tissue of three oak (*Quercus*) species. *Journal of Arboriculture* **31**, 215.
- Percival GC and Sheriffs CN (2002) Identification of drought-tolerant woody perennials using chlorophyll fluorescence. *Journal of Arboriculture* **28**, 215–223.
- Perin G, Bellan A, Segalla A, Meneghesso A, Alboresi A and Morosinotto T (2015) Generation of random mutants to improve light-use efficiency of *Nannochloropsis gaditana* cultures for biofuel production. *Biotechnology for Biofuels* **8**, 161.
- Pisciotta JM, Zou Y and Baskakov IV (2010) Light-dependent electrogenic activity of cyanobacteria. *PLoS One* **5**, e10821.
- Rajpurohit AS, Allard F, Rajpurohit S, Sharma R, Teixeira GDC, Mousis O and Kamlesh R (2018) Exploring the stellar properties of M dwarfs with high-resolution spectroscopy from the optical to the near-infrared. *Astronomy and Astrophysics Supplement Series* **620**, A180.
- Richey-Yowell T, Shkolnik EL, Schneider AC, Osby E, Barman T and Meadows VS (2019) HAZMAT. V. The ultraviolet and X-ray evolution of K stars. *ApJ* **872**, 17.
- Sattari Vayghan H, Tavalaei S, Grillon A, Meyer L, Ballabani G, Glauser G and Longoni P (2020) Growth temperature influence on lipids and photosynthesis in *Lepidium sativum*. *Frontiers in Plant Science* **11**, 745.
- Scalo J, Kaltenecker L, Segura A, Fridlund M, Ribas I, Kulikov YN, Grenfell JL, Rauer H, Odert P, Leitzinger M, Selsis F, Khodachenko ML, Eiroa C, Kasting J and Lammer H (2007) M stars as targets for terrestrial exoplanet searches and biosignature detection. *Astrobiology* **7**, 85–166.
- Schopf JW and Packer BM (1987) Early Archean (3.3-billion to 3.5-billion-year-old) microfossils from Warrawoona Group, Australia. *Science* **237**, 70–73.
- Schulze-Makuch D, Heller R and Guinan E (2020) In search for a planet better than Earth: top contenders for a superhabitable world. *Astrobiology* **20**, 1394–1404.
- Villanueva GL, Smith MD, Protopapa S, Faggi S and Mandell AM (2018) Planetary spectrum generator: an accurate online radiative transfer suite for atmospheres, comets, small bodies and exoplanets. *Journal of Quantitative Spectroscopy and Radiative Transfer* **217**, 86–104.
- Wadhwa S, Panwar MS, Agrawal A, Saini N and Patidar LPL (2012) A review on pharmacognostical study of *Lepidium sativum*. *Advance Research in Pharmaceuticals and Biologicals* **2**, 316323.
- Walker JC (1985) Carbon dioxide on the early Earth. *Origins of Life and Evolution of Biospheres* **16**, 117–127.
- Welander NT and Ottosson B (1997) Influence of photosynthetic photon flux density on growth and transpiration in seedlings of *Fagus sylvatica*. *Tree Physiology* **17**, 133–140.
- Williams DR (2013) *Sun Fact Sheet*. Greenbelt, MD: NASA Goddard Space Flight Center. Available at: <https://nssdc.gsfc.nasa.gov/planetary/factsheet/sunfact.html> (Accessed 9 August 2023).
- Wolfe A, Guinan EF, Datin KM, DeWarf LE and Engle SG (2010) Are main-sequence K-type stars the ‘Goldilocks’ stars for hosting long-term habitable planets. *AAS* **215**, 423.10.
- Zakhochay VA (2013) Lifetimes of stars in the main sequence and the maximum mass of stars in the galactic disk. *Kinematics and Physics of Celestial Bodies* **29**, 195–201.